C. R. Physique 14 (2013) 141–148

Contents lists available at SciVerse ScienceDirect

Comptes Rendus Physique

www.sciencedirect.com

Crystal growth / Croissance cristalline

Twinning occurrence and grain competition in multi-crystalline silicon during solidification

Maclage et compétition de grains dans le silicium multi-cristallin durant la solidification

Amina Tandjaoui [a,b,*], Nathalie Mangelinck-Noel [a,b], Guillaume Reinhart [a,b], Bernard Billia [a,b], Xavier Guichard [c]

[a] *Aix-Marseille Université, campus Saint-Jérôme, case 142, 13397 Marseille cedex 20, France*
[b] *CNRS, IM2NP, UMR CNRS 7334, campus Saint-Jérôme, case 142, 13397 Marseille cedex 20, France*
[c] *ESRF, polygone scientifique Louis-Néel, BP220, 38043 Grenoble cedex, France*

A R T I C L E   I N F O

Article history:
Available online 14 February 2013

Keywords:
Silicon
Solidification
X-ray radiography
Synchrotron
Twins
Grain competition

Mots-clés :
Silicium
Solidification
Radiographie X
Synchrotron
Macles
Compétition de grains

A B S T R A C T

Multi-crystalline silicon solidification is investigated by performing directional solidification experiments. Twinning phenomenon has been identified and observed in situ and in real time during the solidification using X-ray synchrotron imaging techniques: radiography and topography. The radiography observations give information on the formation, birth localized at the interface and evolution of the twins during solidification. The topography results give further information on the grain arrangement and on new grains in twinned position and grain growth competition. We have evidenced two twinning mechanisms: the first is the multiple twin formations during the growth of one grain. The second is the nucleation of a grain in twinned position at the bottom of a grain boundary groove.

R É S U M É

La solidification du silicium multi-cristallin a été étudiée en menant à bien des expériences de solidification dirigée. Le phénomène de maclage a été identifié et observé in situ et en temps réel pendant la solidification, en utilisant des techniques d'imagerie X synchrotron : radiographie et topographie. Les observations par radiographie donnent des informations concernant la formation, la localisation à l'interface et l'évolution des macles au cours de la solidification. Les résultats de topographie donnent des informations complémentaires sur l'arrangement des grains et sur la compétition de croissance des macles et des grains. Nous avons montré l'existence de deux mécanismes de maclage : la formation de macles multiples pendant la croissance d'un grain et la germination d'une macle unique dans le sillon d'un joint de grains.

1. Introduction

The elaboration process of multi-crystalline (mc) silicon has a significant effect on the photovoltaic properties and in particular the solidification step generates a great amount of defects. Thus, a precise control of the solidification of mc-silicon

* Corresponding author at: Aix-Marseille Université, campus Saint-Jérôme, case 142, 13397 Marseille cedex 20, France.
E-mail address: amina.tandjaoui@im2np.fr (A. Tandjaoui).

1631-0705/$ – see front matter
http://dx.doi.org/10.1016/j.crhy.2012.12.001

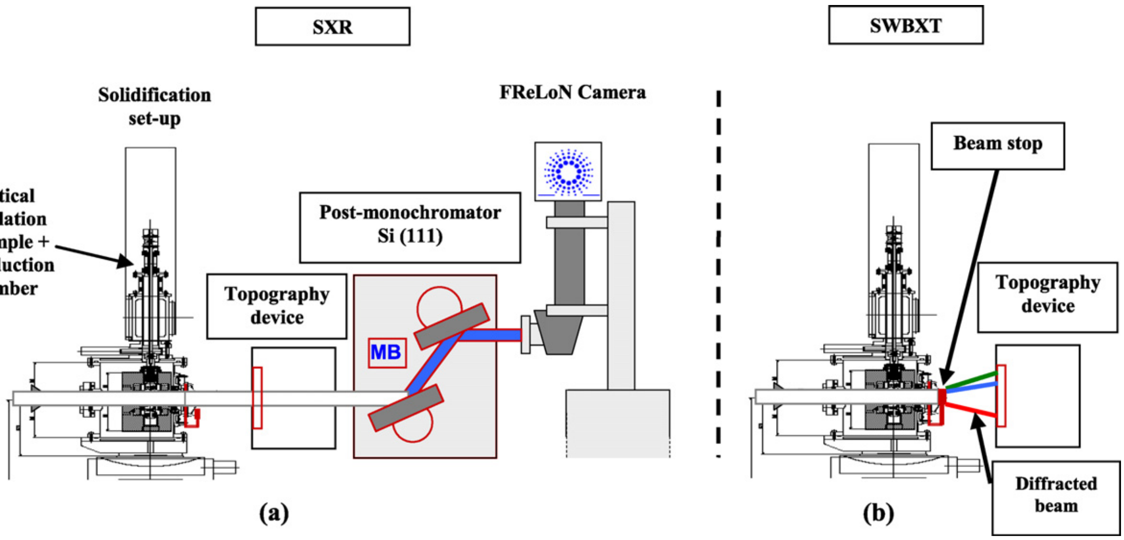

Fig. 1. Schematic drawing describing the two imaging techniques used: (a) X-ray radiography mode; (b) X-ray topography mode.

is needed to improve the crystalline quality and consequently the efficiency of mc-silicon solar cells [1]. With this objective, the formation of grains, twins and dislocations must be understood and controlled.

In general, a silicon ingot with larger scale grains is preferred for increasing the minority carrier lifetime [2–5]. With this perspective, Fujiwara et al. [6] proposed a method to reduce the number of grains by growing silicon dendrites and, other authors improved the control of new nucleations and grain competition during directional solidification of mc-Si [7].

Dislocations are related to stress during the solidification and are also deleterious for photovoltaic properties [8]. Recently, Nakajima et al. [9] developed an experimental technique by growing a silicon ingot with a non-contact crucible method, to reduce the stresses thus reducing the number of resulting dislocations.

Twinning is another essential feature of the solidification of mc-Si ingots and is very frequent. Multiple twinning modifies the final grain structure after solidification and has an effect on the distribution of the crystallographic orientations of the grains in the ingot [10]. Recently, it was shown that grains showing twins are less prone to the formation of dislocations thus insuring better photovoltaic properties [7,11].

We recently developed a device devoted to the characterization of the solidification of silicon by synchrotron X-ray imaging techniques, in situ and in real time. We combined two complementary techniques: X-ray radiography giving information on the solid/liquid interface and its features, and X-ray topography giving information on the growing grains, their crystallographic orientations and additional phenomena such as strains and defects [12]. In the present paper, results concerning the twin formation during solidification are discussed.

Fujiwara et al. [13] developed an optical imaging technique to reveal the solid–liquid silicon interface during growth. They suggested a model for twins followed by facetted dendrite growth by in situ and post mortem observations [14]. Our observations detailed in the following show that the twinning phenomenon occurred in two distinctive ways in our experiments: multiple twinning at grain growth interface during solidification or nucleation of a single twin in a grain boundary groove.

In this paper, we report the details of both mechanisms and the concomitant phenomena arising as grain competition for instance.

2. Experimental device

The Bridgman furnace and its environment are designed to be compatible with X-ray synchrotron imaging techniques. Experiments are performed at beam line BM05 at the ESRF (European Synchrotron Radiation Facility).

The sample/crucible set is introduced in the furnace perpendicularly to the X-ray beam. The crucibles are made of pyrolytic boron nitride, and the samples studied are from several silicon grades: high quality silicon (6N), Metallurgical Grade silicon (MG-Si), Solar Grade silicon (SoG-Si) and Upgraded Metallurgical Grade silicon (UMG-Si). These samples are cut and polished and have dimensions of: 40×6 mm^2 for the surface and 300 μm in thickness.

During its solidification, the sample which is inserted in the furnace is illuminated by synchrotron white beam radiation. In radiography mode, the transmitted beam is monochromated at an energy $E = 17.5$ KeV by a post-specimen monochromator and collected by a FReLoN (Fast Readout–Low Noise) CCD camera (Fig. 1(a)). The typical exposure time for a radiography image is from 0.5 s to 1 s. The camera pixel resolution is 7.46 μm and the field of view is fixed to 6×8 mm^2. Thus, we can observe the dynamic evolution of the solid/liquid interface during the solidification.

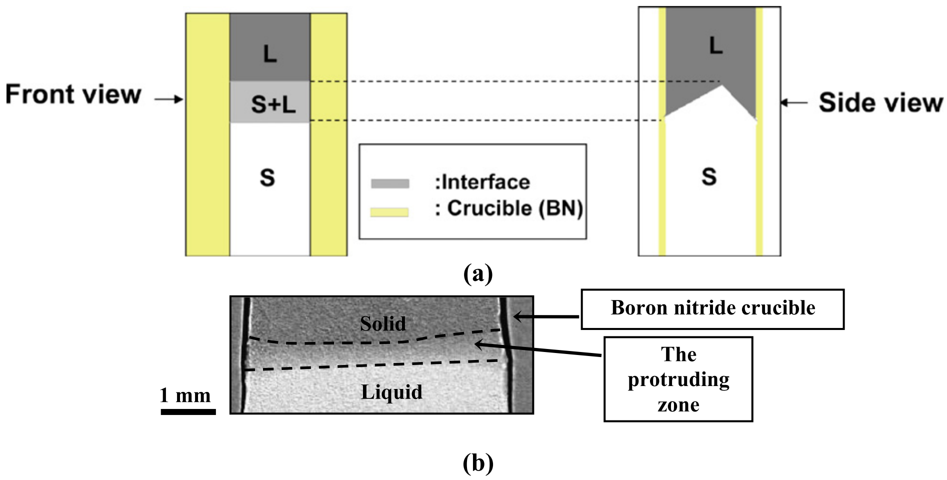

Fig. 2. (a) Schematic drawing describing the division pixel by pixel of the current image by the first after setting the solidification parameters. (b) X-ray radiography image of pixel by pixel division of the current image by the first image (SoG-Si solidifying under thermal gradient $G = 12$ K/cm and cooling rate. $R = 0.2$ K/min).

In the X-ray topography mode, the sample is also illuminated by the white beam but the directly transmitted beam is stopped by a beam-stop made of copper and the diffracted beams are collected on AGFA structuric D3-SC X-ray sensitive films (12.5×17.6 cm^2). The topography device allows us to record up to 30 films by experiment so that we can follow the growth of the grains accurately (Fig. 1(b)). These films collect many spots called topographs giving information on the grain structure, the crystallographic orientation and the phenomena occurring during solidification such as strains and defects. More details about the technique can be found in [12].

The X-ray radiography imagery is based on absorption differences of the X-ray beam. Images collected are processed to allow us to distinguish the solid/liquid interface and its features. Indeed, the difference in density between solid and liquid silicon is small, so that image treatment is necessary. Two image processing methods are used to obtain complementary information on the solid–liquid interface shape and dynamics:

- Pixel by pixel division of the current image by the first image after starting the cooling. By these treatments the solid appears in white and the liquid in grey (Fig. 2(a)). This treatment reveals a light grey zone which corresponds to a protruding solid zone in the liquid. It shows that the interface is not flat and not perpendicular to the crucible wall in the thickness direction.
- Pixel by pixel division of successive images reveals in more details the morphology of the solid/liquid interface, and particularly, the facetted or rough character of the solid/liquid interface (Fig. 3). Fig. 3(a) shows a scheme of this image treatment. The blue dashes limit the solid/liquid interface in previous image and the red dashes the solid/liquid interface in the next image. In summary, we will perceive four white lines on the processed images (representing by two blue and two red on Fig. 3(a)).

Melting and solidification of silicon sample are achieved in a Bridgman furnace by increasing, respectively decreasing the temperatures of the two graphite heaters instead of the translation system. Indeed, the solid/liquid interface with the pulling experiments is almost indistinguishable due to the need of image treatments as explained above.

3. Results and discussion

3.1. Multiple twinning formation

Fig. 3 shows processed radiography images of a MG-Si sample solidifying under a thermal gradient $G = 15$ K/cm and with a cooling rate $R = 1$ K/min applied on both heaters. The average interface velocity was measured and is $V_g = 11$ μm/s. On these images we can observe diffracting twins. The black contrast corresponds to planes that satisfy the Bragg condition for the selected energy (17.5 keV). As a consequence, there is extinction in the contrast corresponding to these planes in the directly transmitted beam. It is worth noting that in radiography mode, twinning may occur in other grains in the silicon sample but if they are not in a crystallographic orientation that satisfies the Bragg condition for the energy of 17.5 KeV of the beam, they do not diffract (i.e. they will not induce loss of beam intensity).

The same phenomenon is relevant for the grains that form the sample. Grains that are not in Bragg position for the selected energy in radiography acquisition (17.5 KeV), will not diffract.

One important feature is that we can distinguish the birth location of these twins, which takes place at the level of the solid/liquid interface at the top of the protruding region (Fig. 4(a)). In the literature, there is still a debate concerning

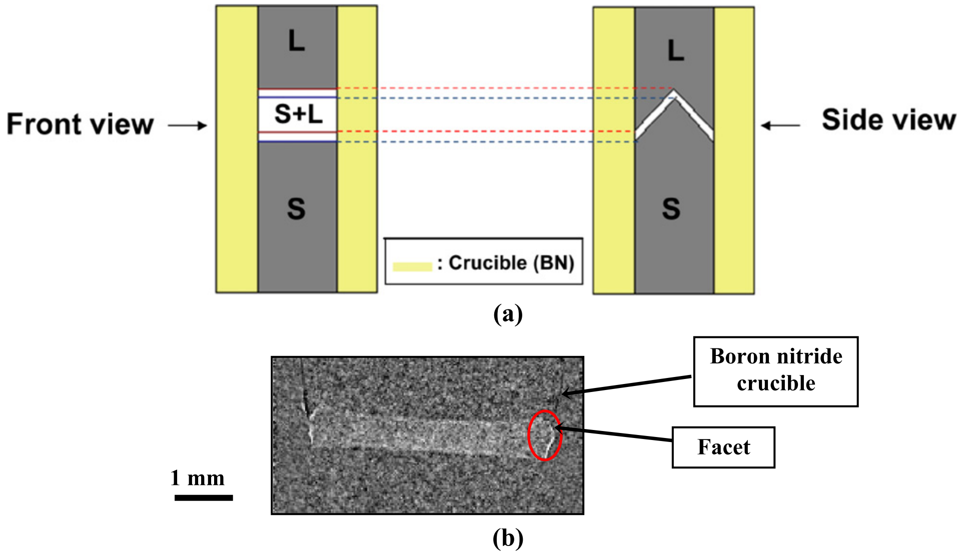

Fig. 3. (a) Schematic drawing describing the division pixel by pixel of two successive images. The blue dashes limit the solid/liquid interface in the previous image and red ones limit the solid/liquid interface in the next image. (b) X-ray radiography image of pixel by pixel division of successive images (SoG-Si solidifying under thermal gradient $G = 11$ K/cm and cooling rate $R = 0.5$ K/min). (For interpretation of the references to color in this figure legend, the reader is referred to the web version of this article.)

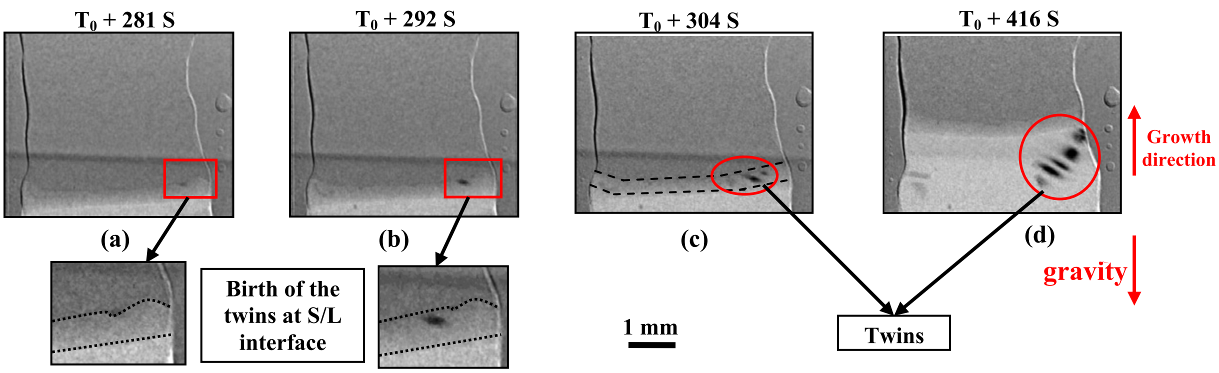

Fig. 4. X-ray radiography images of twin formation during solidification in a MG-Si solidifying under a thermal gradient $G = 15$ K/cm, at a cooling rate $R = 1$ K/min applied on both heaters at t_0: (a) and (b) birth of the twins at the S/L interface; (c) and (d) multiple repetitive twinning.

the formation of twins [15,16] and we prove here that the twin we observed form at the solid/liquid interface during solidification and not in the solid just below the interface.

The hachured aspect seen in Fig. 4(d) is the same as typically observed in numerous mc-Si grains in wafers from directionally solidified ingots. It is the sign of multiple twinning. With X-ray radiography, we also show that the twins are repeatedly forming with the same orientation (because they diffract in the Bragg position) with very regular spacing. It is worth noting that we observe this behavior and twin formation in numerous experiments, for different cooling rates and, for different silicon grades. In our experiments not all shown in this paper, we observe that multiple twining formation is more frequent in high purity silicon (6N) material.

We complete the study of multiple twins with topography results. Fig. 5(a) shows a topographic film recorded during the solidification of a 6N purity silicon solidifying under a thermal gradient $G = 16$ K/cm and a cooling rate $R = 0.2$ K/min on both heaters. The spot highlighted by a circle marks a reflection of a plane of one growing grain. We record topographs at several instants of the solidification and we can thus follow the time evolution on this grain Fig. 5(b). The hachured aspect indicates again the twinned planes. The blank part of the grain corresponds to the twins that are disoriented in comparison to the grain orientation corresponding to this reflection. Thus, these twins diffract at other positions on the topographic film.

The topographs confirm that repetitive twins are formed at the solid/liquid interface (see circle Fig. 5(b)). Further analyses are underway to determine the orientation of the grains and twins by indexing the diffraction diagrams.

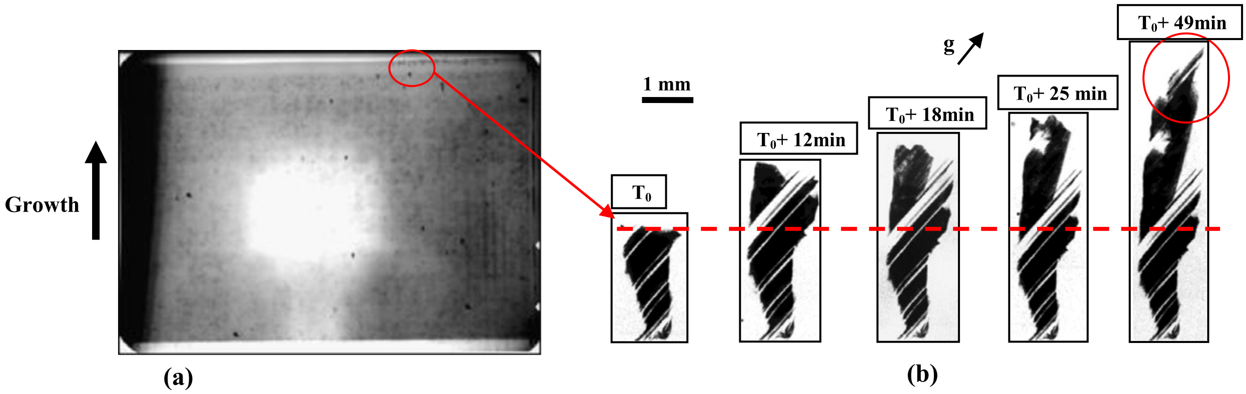

Fig. 5. Multiple twinning, (a) Topographic film of the solidification of 6N purity Si solidifying under a thermal gradient $G = 16$ K/cm and cooling rate $R = 0.2$ K/min. (b) Time evolution of one grain during the solidification. T_0 is the beginning of cooling. g is the diffraction vector.

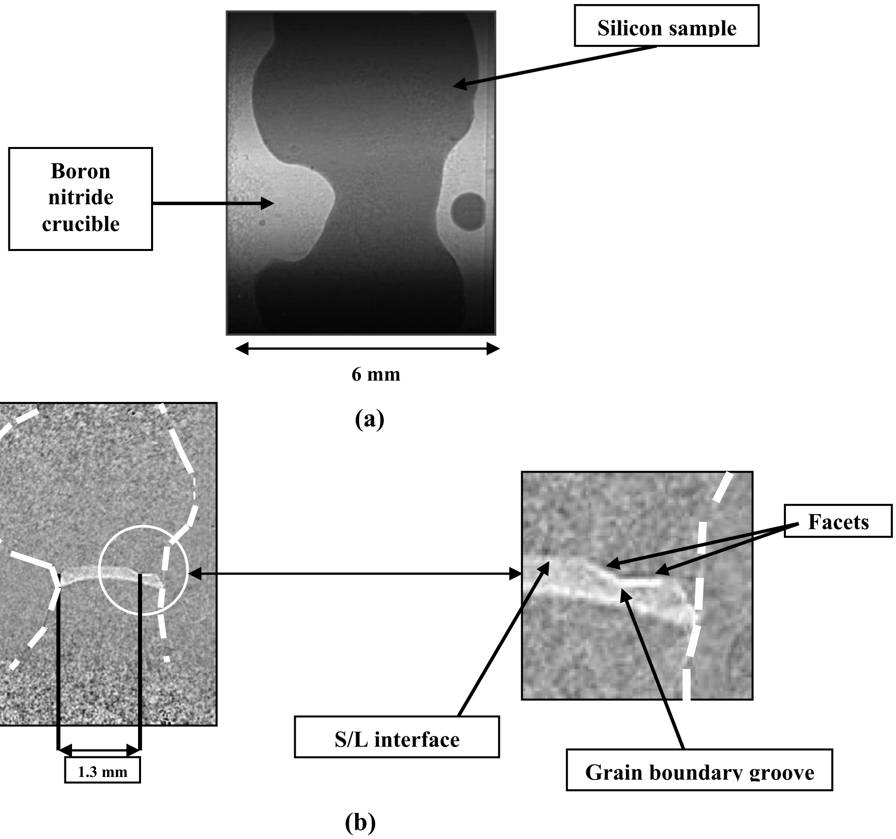

Fig. 6. X-ray radiography image of an UMG-Si sample solidifying under a thermal gradient $G = 16$ K/cm and at a cooling rate $R = 0.4$ K/min on both heaters: (a) Raw image. (b) Division of successive images: groove located at the solid/liquid interface at 1.3 mm from the left side of the sample. The white dashes limit the silicon sample.

3.2. Twinning nucleation and subsequent grain competition

Fig. 6 show a raw radiography image and processed radiography image of an UMG-Si sample during solidification under a thermal gradient $G = 16$ K/cm and at a cooling rate $R = 0.4$ K/min applied on both heaters.

On the X-ray radiography images, we observe a groove at the solid/liquid interface, which is repeatedly appearing during all the solidification experiment (Fig. 6(b)).

The groove at the solid/liquid interface is in fact a grain boundary groove widening repetitively. Indeed, Fig. 6 show only one image at a precise instant of the solidification experiment. When we follow the growth of this sample during all the

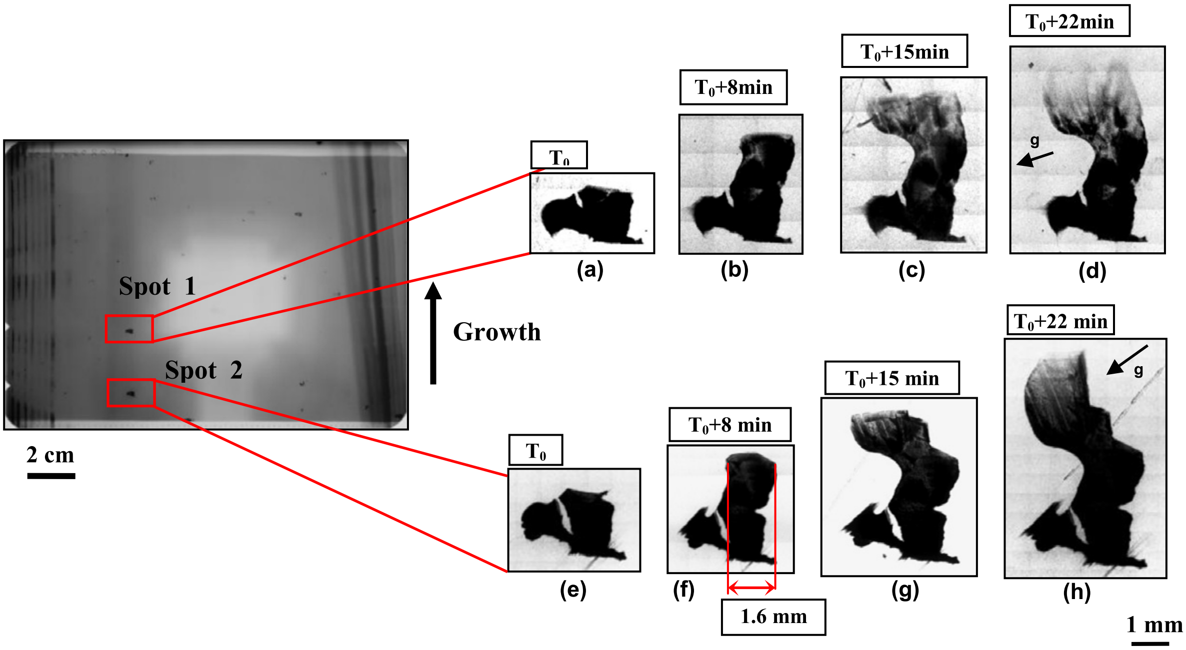

Fig. 7. X-ray topography results of an UMG-Si sample solidifying under thermal gradient $G = 16$ K/cm and at a cooling rate $R = 0.4$ K/min on both heaters. Sequences of two spots during the solidification experiment: (a) and (e) $T = T_0$: start of the solidification, (b) and (f) $T = T_0 + 8$ min: vertical growth, (c) and (g) $T = T_0 + 15$ min: lateral growth, (d) and (h) $T = T_0 + 22$ min.

experiment, we notice that this groove is observed clearly on some images only. This is confirmed by the complementary topography results. Fig. 7 shows two spots highlighted by red rectangles at different positions of the same topographic film for the same experiment as in Fig. 5. On this figure, we also present the time evolution of these two spots during the solidification experiment. These diffraction spots (Fig. 7) only correspond to a part of the silicon sample (Fig. 6) indicating that we have several grains growing at the interface with different crystallographic orientations so that their diffraction spots are located at other positions of the film. Moreover, the width of the grain is measured on the topograph and is about 1.6 mm (e.g. on Fig. 7(f)). This value is comparable to the distance measured between the groove occurrence position and the left side of the sample (1.3 mm) on the radiography image (Fig. 6). Thus, we can conclude that the groove observed Fig. 6 marks a grain boundary position. Deformed images of the grains due to strains are obtained in topography which can explain the small discrepancy between the two values measured on the topography and on the radiography.

From Fig. 7(a) to 7(b), the two spots reflect the vertical growth of the left hand side of the sample in the radiography images. From Figs. 7(c) and (g), we can observe the lateral growth to the left due to the particular shape of the silicon sample (Fig. 6) that shows a width increase. On the other hand, the sample as shown in Fig. 6 is formed by several grains oriented differently. The grains that appear in topograph of Fig. 7 correspond to the left hand side of the sample. We can notice that the right side of the sample is missing on the considered spots.

During growth the left side grains couldn't develop larger than those shown on the spots because there are in competition with the grains of the right side. So, their lateral growth is blocked on the right.

The image of Spot 1 is wider in the right lateral direction in comparison with Spot 2 at the same instant (Fig. 7). This is an evidence of the existence of a twin forming during solidification. Indeed, the definition of a twin is to have a common plane with the neighbor grain which is exactly what is shown thanks to topography technique on the common reflection: Spot 1 in Fig. 7. The corresponding grain in twinned position spot diffracts at another position on the topographic film (Spot 3 in Fig. 8). We have also recorded its growth *in situ* and in real time. The peculiarity of this grain is its V-shape corresponding to the grain boundary groove shape on the radiography image which suggests that this grain has nucleated in this groove.

In the following stage, grains that form Spot 2 and neighbor grain in twinned position are in growth competition. The consequence is the occurrence of the particular shape of the pre-existing grain characterized by the formation of steps after the nucleation of the twin (Spot 2 in Figs. 7(g) and (h)).

The occurrence of these large steps shows that the grains that form Spot 1 in Fig. 8 and the grain that nucleated in the grain boundary groove which is in twinned position (Spot 3) are alternatively growing faster in the lateral direction comparatively to each other during the solidification sequence, see Fig. 7. At least two mechanisms can favor the growth of one grain relatively to the other and could compete in our experiments: their crystallographic orientations and the local solidification conditions (e.g. local isotherm curvature). Moreover, more analyses are underway to deepen the understanding about the nucleation of grains in twinned position and of grains in grain boundary grooves.

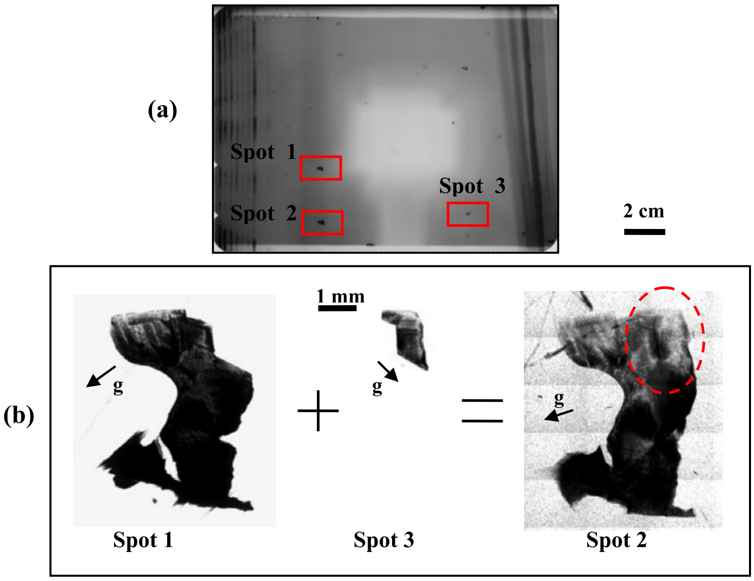

Fig. 8. X-ray topography results of an UMG-Si sample solidifying under thermal gradient $G = 16$ K/cm and at a cooling rate $R = 0.4$ K/min on both heaters: (a) Topographic film at instant T_0 and position of Spots 1–3. (b) Diffraction of three spots at instant $T_0 + 15$ min. Spot 3 is the spot corresponding to the nucleated twin grain which is missing on Spot 1 when compared to Spot 2.

4. Conclusion

We observe and characterize two mechanisms of twin formation. One mechanism leads to the formation of repetitive twins widely observed in silicon ingots. In that case, twins are formed at the solid–liquid interface, have the same crystallographic orientation and are regularly spaced. Moreover, in our experiments, the multiple twinning is observed more frequently in high purity silicon material.

For the other mechanism, a grain in twinned position is formed at a grain boundary groove and enters in growth competition with the pre-existing grains in the silicon sample.

The indexation of the topographs giving information on the grain orientations and consequently on the orientation of the twinning planes are under way. More experiments on different silicon grades are also foreseen to relate more precisely the twinning occurrence to the impurities amount.

Acknowledgements

This work was part of the project SiX funded by ANR (Program HABISOL). Partners from ESRF (European Synchrotron Radiation Facility) and in particular from beam line BM05 are deeply acknowledged for support during the experiments and fruitful discussions.

References

[1] L. Arnberg, et al., State-of-the-art growth of silicon for PV applications, J. Cryst. Growth 360 (2012) 56–60.
[2] H.Y. Wanget, et al., Microstructures of Si multicrystals and their impact on minority carrier diffusion length, Acta Mater. 57 (2009) 3268.
[3] R. Bairava Ganesha, et al., Growth and characterization of multi-crystalline silicon ingots by directional solidification for solar cell applications, Energy Procedia 8 (2011) 371.
[4] T.Y. Wang, et al., Grain control using spot cooling in multi-crystalline silicon crystal growth, J. Cryst. Growth 311 (2009) 263.
[5] V. Osinniy, et al., Factors limiting minority carrier lifetime in solar grade silicon produced by metallurgical route, Sol. Energy Mater. Sol. Cells 95 (2011) 564.
[6] K. Fujiwara, et al., Directional growth method to obtain high quality polycrystalline silicon from its melt, J. Cryst. Growth 292 (2006) 282.
[7] C.W. Lan, et al., Grain control in directional solidification of photovoltaic silicon, J. Cryst. Growth (2012), in press.
[8] N. Usami, et al., Implementation of faceted dendrite growth on floating cast method to realize high-quality multicrystalline Si ingot for solar cells, J. Appl. Phys. 109 (2011).
[9] K. Nakajima, et al., Growth of multi-crystalline Si ingots using non-contact crucible method for reduction of stress, J. Cryst. Growth 344 (2012) 6.
[10] T. Duffar, in: Recent Research Developments in Crystal Growth, vol. 5, 2010, pp. 61–113.
[11] G. Stokkan, Acta Mater. 58 (2010) 3223–3229.
[12] A. Tandjaoui, et al., Real time observation of the directional solidification of multi-crystalline silicon: X-ray imaging characterization, Energy Procedia 27 (2012) 82–87.

[13] K. Fujiwara, et al., In situ observations of crystal growth behavior of silicon melt, J. Cryst. Growth 243 (2002) 275.
[14] K. Fujiwara, et al., Formation mechanism of parallel twins related to Si-facetted dendrite growth, Scr. Mater. 57 (2007) 81.
[15] T. Duffar, A. Nadri, Scr. Mater. 72 (2010) 955–960.
[16] J. Pohl, et al., Formation of parallel (111) twin boundaries in silicon growth from the melt explained by molecular dynamics simulations, J. Cryst. Growth 312 (2010) 1411.